Adaptive Sensing for Terrain Aided Navigation*

H. J. S. Feder, J. J. Leonard, and C. M. Smith
Department of Ocean Engineering
Massachusetts Institute of Technology
Cambridge, MA 02139, USA
{feder,jleonard,cmsmith}@deslab.mit.edu

Abstract

This paper demonstrates experiments for performing adaptive terrain aided navigation in the context of autonomous underwater vehicles (AUVs) equipped with sonar. The experiments were conducted using a 675 kHz sector scan sonar mounted on a planar robotic positioning system in a 3.0 by 9.0 by 1.0 meter testing tank, enabling controlled and repeatable scenarios. The objective of the adaptive stochastic mapping algorithm is to enable feature-based terrain aided navigation of AUVs in environments where no a priori map is available. The approach assumes that distinctive, point-like features can be extracted from vehicle sensor data. A dead-reckoning error model is incorporated to simulate an AUV's navigation system error growth. An adaptation step based on maximizing the Fisher information gained by the next action of the sensor is coupled with the stochastic mapping algorithm to yield more precise position estimates for features in the environment and the vehicle.

1 Introduction

Terrain-aided navigation techniques offer promise to enable AUV missions that would otherwise not be possible, due to the impracticality of deploying acoustic beacons or surfacing for GPS resets. The goal of terrain-aided navigation (also called geophysical navigation) is to match vehicle sensor data to an *a priori* map of the environment to deduce the vehicle position. The idea has its origins in techniques of navigating at sea using depth soundings that have been in use for centuries. Perhaps the most well-known system for terrain-aided navigation is the terrain contour matching system for localization of airborne vehicles using radar altimeter data [3]. For AUV navigation, geophysical parameters that might be employed for terrain-aided navigation include gravity, magnetic field and bathymetry [2, 4].

Several promising algorithms for matching data to an *a priori* map have been developed [4, 13, 5]. One can distinguish between techniques which are feature-based and field-based. In field-based geophysical navigation, the goal is to match sensor data with a continuous, *a priori* map of a geophysical parameter whose value is known at all locations in space. Accurate localization will require that a map of sufficiently high resolution is available and that there is sufficient spatial variation in the parameter(s) being measured. If distinctive environmental features are present in the environment, and can be detected from vehicle sensor data, then a feature-based approach offers the potential of accurate positioning with a compact representation. In addition, operation in an environment in which there is no *a priori* map can be addressed in a feature-based approach using algorithms for concurrent mapping and localization (CML) [11].

The goal of concurrent mapping and localization is for the AUV to build a map of its environment and to use that map to navigate in real time. CML has been an important goal in the robotics community, due to its critical importance for mobile robot applications [12, 8]. The problem of CML presents a wide range of theoretical challenges, including feature extraction, state estimation, data association, computational complexity, map representation, and map maintenance in dynamic environments. Adaptive sensing strategies can assist greatly in addressing these challenges to realize improved CML performance. Adaptive sensing can save time and energy and can reduce the amount of data that needs to be acquired and processed to achieve a given level of performance.

In our previous work, we have developed a feature-based approach to concurrent mapping and localization for AUVs and presented CML results using simulated forward look sonar data [11, 10]. In addition, we

*To appear in IEEE Oceans 1998, Nice, France.

have developed an adaptive sensing method for CML, defined in terms of the Fisher Information, and tested it in simulation and with a land robot equipped with a scanning sonar [1]. This paper builds on this earlier work by describing an experimental implementation of adaptive CML with underwater sonar data using a 675 kHz sector scan sonar mounted on a planar robotic positioning system in a 3.0 by 9.0 by 1.0 meter testing tank. In these experiments, the motion and scanning directions of the sensor are chosen adaptively to optimize the performance of CML. The metric for adaptive sensing differs from previous work by making explicit the tradeoff between the growth of uncertainty due to motion of the vehicle and the gain of information provided by sensor measurements of environmental features.

The structure of this paper is as follows: Section 2 summarizes the stochastic mapping algorithm for CML. Section 3 describes a method for performing CML adaptively based on the Fisher Information. Section 4 describes the experimental setup consisting of a sector-scan sonar system mounted on a robotic positioning system in a testing tank using simple geometric objects as features. Section 5 presents experimental results that demonstrate adaptive feature-based concurrent mapping and localization with real data. Finally, Section 6 concludes the paper by summarizing our results and discussing future research topics.

2 Stochastic mapping

The algorithm used in our CML experiments is an enhanced version of the stochastic mapping method first published by Smith, Self, and Cheeseman [12]. The robot senses features in the environment through range and bearing measurements relative to the AUV's current state (position and orientation). These measurements are used to create a map of the environment and concurrently to localize the vehicle.

We use $\mathbf{x}[k] = \hat{\mathbf{x}}_{k|k} + \tilde{\mathbf{x}}[k]$ to represent the system state vector $\mathbf{x} = [\mathbf{x}_r^T \ \mathbf{x}_1^T \ldots \mathbf{x}_N^T]^T$, where $\mathbf{x}_r$ and $\mathbf{x}_1 \ldots \mathbf{x}_N$ are the robot and feature states, respectively, $\hat{\mathbf{x}}$ is the estimated state vector, and $\tilde{\mathbf{x}}$ is the error estimate. Measurements are taken every $t = kT$ seconds, where T is a constant period and k is a discrete time index. The estimate error covariance, $\mathbf{P}_{k|k} = E\{\tilde{\mathbf{x}}[k]\tilde{\mathbf{x}}^T[k]\}$, of the system takes the form

$$\mathbf{P}_{k|k} = \begin{bmatrix} \mathbf{P}_{rr} & \mathbf{P}_{r1} & \cdots & \mathbf{P}_{rN} \\ \mathbf{P}_{1r} & \mathbf{P}_{11} & \cdots & \mathbf{P}_{1N} \\ \vdots & \vdots & \ddots & \vdots \\ \mathbf{P}_{Nr} & \mathbf{P}_{N1} & \cdots & \mathbf{P}_{NN} \end{bmatrix}_{k|k} . \quad (1)$$

Thus, the robot and the map are represented by a single state vector, $\mathbf{x}$, with an associated estimate error covariance $\mathbf{P}$ at each time step. We denote the vehicle's state by $\mathbf{x}_r = [x_r \ y_r \ \phi]^T$ and the control input to the vehicle is given by $\mathbf{u}[k]$. The state transition function, $\mathbf{f}()$, is given by

$$\mathbf{x}[k+1] = \mathbf{f}(\mathbf{x}[k], \mathbf{u}[k]) + \mathbf{d}_{\mathbf{x}}(\mathbf{u}[k]), \quad (2)$$

where $\mathbf{d}_{\mathbf{x}}(\mathbf{u}[k])$ is a white, Gaussian random process independent of $\mathbf{x}[0]$, with magnitude dependent on the control input $\mathbf{u}[k]$.

The observation model $\mathbf{h}()$ for the system is given by

$$\mathbf{z}[k] = \mathbf{h}(\mathbf{x}[k]) + \mathbf{d}_{\mathbf{z}}, \quad (3)$$

where $\mathbf{z}[k]$ is the observation vector of range and bearing measurements. The observation model, $\mathbf{h}()$, defines the nonlinear coordinate transformation from state to observation coordinates. The stochastic process $\mathbf{d}_{\mathbf{z}}$, is assumed to be white, Gaussian, and independent of $\mathbf{x}[0]$ and $\mathbf{d}_{\mathbf{x}}$, and has covariance $\mathbf{R}$.

The predicted current state of the system, $\hat{\mathbf{x}}_{k+1|k}$, is found by taking expectations over Equation (2). The estimated state and covariances are propagated through an extended Kalman filter (EKF). Data association is performed by finding the group of sonar returns of nearly the same range that is closest to each track. It is assumed that a sonar return originates from not more than one feature. After the closest return to each feature is found, this return is gated with the estimated feature position.

Each cycle in the SM algorithm consists of the following steps:

1. **state projection**: the system state (vehicle and features) is projected to the next time step using the state transition model $\mathbf{f}()$, along with the actions (control input) $\mathbf{u}[k]$;

2. **gating**: the closest feature to each new measurement is determined and gated with the feature and non-matching measurements are stored; and

3. **state update**: re-observed features update the vehicle and feature tracks using the EKF.

3 Adaptive sensing

We define $\mathbf{Z}^k \equiv \mathbf{z}[k], \ldots, \mathbf{z}[0]$ to be the set of measurements from time step 0 to the current time step k. As $\mathbf{x}[k]$ is unknown, we can only estimate it by $\hat{\mathbf{x}}[k]$ given all the measurements $\mathbf{Z}^k$. In order to perform adaptive terrain aided navigation, we are interested in the information that can be gained from taking the measurement $\mathbf{z}[k]$. This can be quantified using the Fisher information:

$$\begin{aligned}\mathbf{I}_{\mathbf{z}}(\mathbf{x})[k|k] = &- \underset{\mathbf{z}}{E}\{\nabla_{\mathbf{x}} \nabla_{\mathbf{x}}^T \ln p(\mathbf{Z}^k|\mathbf{x}[k])\} \\ &- \underset{\mathbf{z}}{E}\{\nabla_{\mathbf{x}} \nabla_{\mathbf{x}}^T \ln p(\mathbf{x})\}.\end{aligned} \tag{4}$$

The information $\mathbf{I}_{\mathbf{z}}(\mathbf{x})[k|k]$ quantifies the information of all the measurements $\mathbf{Z}^k$ as well as the information in the prior $p(\mathbf{x})$, such as, knowledge about the uncertainty of our vehicle and sonar model.

Under the assumption that the EKF is a good approximation to an *efficient estimator*, the information $\mathbf{I}_{\mathbf{z}}(\mathbf{x})[k|k]$ is well approximated by the inverse of the error covariance $\mathbf{P}_{k|k}$ of the system. Thus, the information of the system at time step k given the prior and all past measurements is readily available to us directly from the EKF. Following the method described in [1], we obtain the transformation that relates the current information $\mathbf{I}_{\mathbf{z}}(\mathbf{x})[k|k]$ to the predicted resulting information $\mathbf{I}_{\mathbf{z}}(\mathbf{x})[k+1|k+1]$ due to an action $\mathbf{u}[k]$. The action that maximizes the information gained can be expressed as:

$$\mathbf{u}[k] = \max_{\mathbf{u}} \arg \mathbf{I}_{k+1|k+1} = \min_{\mathbf{u}} \arg \mathbf{P}_{k+1|k+1}. \tag{5}$$

The information is a matrix and we require a metric to quantify the information. Further, it is desired that this metric have a simple physical interpretation.

The question of defining a metric for adaptive sensing has been considered by previous researchers in different contexts. Manyika utilized a metric based on entropy to define a scalar cost function that was used in a multi-sensor robot localization system [6]. Singh has developed an entropic measure for grid-based mapping and implemented it with the Autonomous Benthic Explorer [9].

For feature-based CML, it is desirable to use a metric that makes explicit the tradeoff between uncertainty in feature locations and uncertainty in the vehicle position estimate. To accomplish this, we define the metric by a cost function $C(\mathbf{P})$, which gives the total area of all the error ellipses, (i.e., highest probability density regions) and is thus a measure of our confidence in our map and robot position [1]. That is,

$$C(\mathbf{P}) = \prod_j \sqrt{\lambda_j(\mathbf{P}_{rr})} + \sum_{i=1}^{N} \prod_j \sqrt{\lambda_j(\mathbf{P}_{ii})}, \tag{6}$$

where $\lambda_j(\cdot)$ is the j-th eigenvalue of its argument. The action to take is obtained by evaluating Equation (6) over the action space of the robot. The SM procedure outlined in Section 2 is modified by adding the following adaptation step:

4 **adaptation step**: determine the next action, $\mathbf{u}[k]$ to take by optimizing Equation (6).

This yields an adaptive stochastic mapping algorithm. This procedure optimizes the information locally at each time step, thus the adaptation step performs a local optimization. Notice, that the action space of the robot is not limited to the the direction the robot can move, as represented by the $\mathbf{u}$ in the stochastic map. Other actions and constraints can readily be included, such as, what measurements should be taken by the sonar.

4 Experimental setup

The adaptive stochastic mapping algorithm described above has been implemented using a narrow-beam 675 kHz sector scan sonar mounted on a planar robotic positioning system, as shown in Figure 3. The positioning system is controlled by a Compumotor AT6450 controller card. The system is mounted on a 3.0 by 9.0 by 1.0 meter testing tank. The system executes on a PC running Matlab and C++ under WindowsNT. The C++ routines perform the interface to the sonar and the AT6450. The stochastic mapping algorithm was implemented in Matlab, which is also used for the the graphical user interface. The Matlab and C++ programs are integrated, resulting in a closed loop system for performing CML. Testing tank experimentation provides a bridge between simulation and trials with real vehicles in the field. Repeatable experiments can be easily performed under identical conditions, and ground truth can be determined to high accuracy.

In our experiments, we envision an underwater vehicle equipped with a sonar that can scan at any direction relative to the vehicle at each time step. Conducting complete 360° scans of the environment at every time step is slow with a mechanically scanned sonar and computational expensive with an electronically scanned sonar. Thus, the sonar was limited to only scan over a limited range of angles, $[-\phi, \phi]$, at

each time step. The sonar was modeled to have a standard deviation in bearing of 5.0° and 2.0 centimeters in range. Between each scan by the sonar, the vehicle can move between 15 cm and 30 cm. The lower limit signifies that there is a minimum speed the vehicle can move at before loosing controllability, while the upper limit signifies the maximum speed of the vehicle. Further, the vehicle is limited to turn a maximum of 30° at each time step relative to its current heading, signifying a minimum turning radius. Further, we assumed that the vehicle was equipped with a dead-reckoning system with an accuracy of 10% of distance traveled and an accuracy of 1.0° in heading.

In performing these experiments, Equation (6) was minimized over the action space of the robot.

5 Experimental results

Figure 4 shows a typical scan taken by the sonar from the origin. The crosses shows individual sonar returns. The circles shows the features (PVC tubes). The dotted circles around the features signify the minimum allowable distance between the vehicle and the features. The triangle shows the position of the sensor. Circular arc features are extracted from the sonar scans using a thresholding technique described in [7].

Figure 1 shows the results of two different experiments. In the first, the sonar scannng angle is set to ±30° and in the second it is restricted to ±7.5°. The estimated path of the sensor is shown in a solid line, while the actual path is shown in a dashed line. The filled disks indicates the locations of the features (PVC tubes). The triangle indicates the final position of the sensor. The ellipses shows the 3 σ contour for the location of the features and the final position of the sensor. The sensor starts out at (0,0) and then adaptively determines the path to take as well as the direction to scan. As can be seen, the algorithm results in "exploratory" behavior. The sensor first moves over to one of the objects, turns, and moves around the second. The experiment illustrated in the bottom of Figure 1 is similar, with the exception that the sonar now is only able to scan an area of $[-7.5°, 7.5°]$ each time step. Again, we can see that exploratory behavior emerges as the sensor attempts to maximize the information it obtains about the environment.

Figure 2 compares the size of the vehicle error ellipse produced by CML with the error ellipse produced by dead-reckoning for the experiment.

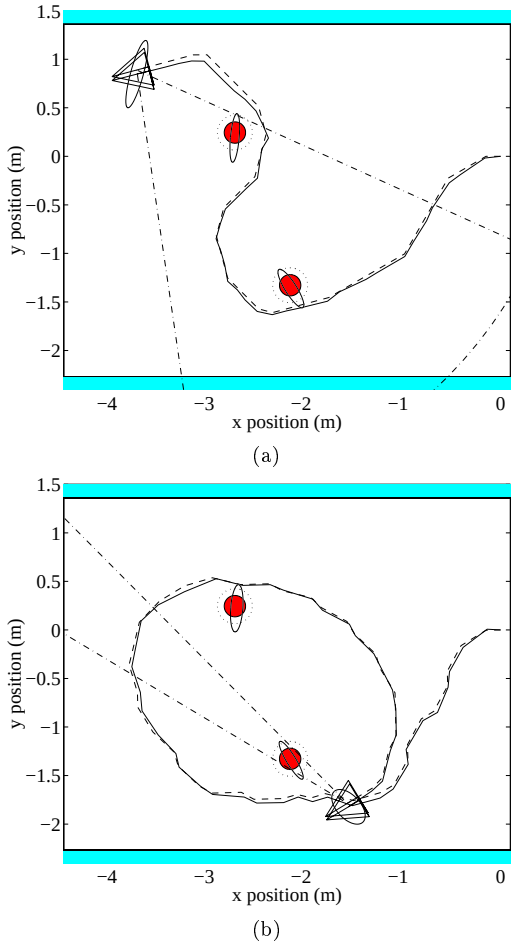

Figure 1: Two different runs of the adaptive feature relative navigation algorithm. In each figure, the solid line shows the estimated path of the sensor and the dashed line shows the actual path. The triangle indicates the final position of the sensor. The filled disks indicate the locations of the features (PVC tubes). The ellipses around the features and the sensor is the 3 σ contour, that is, the 99% highest confidence region. The sonar view is indicated by the dashed-dotted line. In the top figure, the sensor had a scanning angle of $[-30°, 30°]$. In the bottom figure, the sensor had a scanning angle of $[-7.5°, 7.5°]$

6 Conclusion

This paper has considered the problem of adaptive sensing for feature-based concurrent mapping and localization by autonomous underwater vehicles. An adaptive sensing metric has been incorporated within a stochastic mapping algorithm and tested via exper-

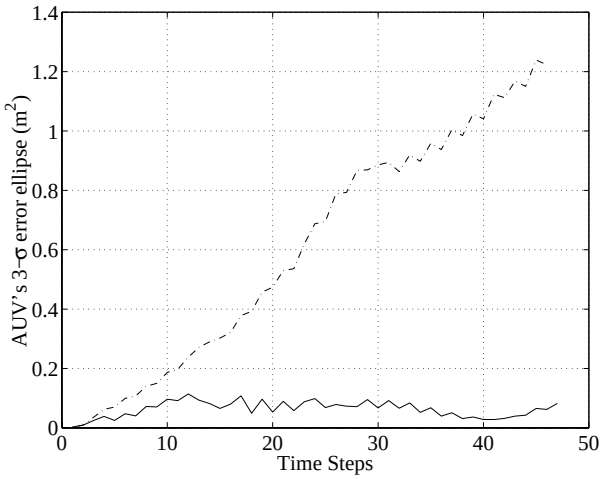

Figure 2: The 3-σ ellipse area of the vehicle as a function of time step for the second run (solid line) along with that for a dead-reckoning run tracing the same path (dashed-dotted line).

iments in a testing tank. This is the first time, to our knowledge, that a feature-based concurrent mapping and localization algorithm has been implemented with underwater sonar data. The system exhibits a behavior in which it selectively explores different objects in the environment.

In future research, we will work to integrate adaptive sensing within a hybrid estimation framework for CML in development in our laboratory [10]. In addition, we will work to perform experiments with more complex objects and to incorporate additional criteria for adaptation to address effects such as occlusion, rough surface scattering, and multiple reflections.

Acknowledgments

This research has been funded in part by the Naval Undersea Warfare Center, Newport, RI, U.S.A. H.J.S.F. acknowledges the support of NFR (Norwegian Research Council) through grant 109338/410. J.J.L. acknowledges the support of the Henry L. and Grace Doherty Assistant Professorship in Ocean Utilization and NSF Career AWARD BES-9733040.

References

[1] H. J. S. Feder, J. J. Leonard, and C. M. Smith. Adaptive concurrent mapping and localization using sonar. In *Proc. IEEE Int. Workshop on Intelligent Robots and Systems*, Victoria, B.C., Canada, October 1998. To Appear.

[2] E. Geyer, P. Creamer, J. D'Appolito, and R. Gains. Characteristics and capabilities of navigation systems for unmanned untethered submersibles. In *Proc. Int. Symp. on Unmanned Untethered Submersible Technology*, pages 320–347, 1987.

[3] R. R. Hatch, J. L. Luber, and J. H. Walker. Fifty years of strike warfare at the Applied Physics Laboratory. *Johns Hopkins APL: Technical Digest*, 13(1):113–124, January-March 1992.

[4] B. Kamgar-Parsi, L. Rosenblum, F. Pipitone, L. Davis, and J. Jones. Toward an automated system for a correctly registered bathymetric chart. *IEEE J. Ocean Engineering*, 14(4):314–325, October 1989.

[5] L. Lucido, B. Popescu, J. Opderbecke, and V. Rigaud. Segmentation of bathymetric profiles and terrain matching for underwater vehicle navigation. In *Proceedings of the second annual World Automation Conference*, Montpellier, France, May 1996.

[6] J. S. Manyika and H. F. Durrant-Whyte. *Data Fusion and Sensor Management: A decentralized information-theoretic approach*. New York: Ellis Horwood, 1994.

[7] B. A. Moran, J. J. Leonard, and C. Chryssostomidis. Curved shape reconstruction using multiple hypothesis tracking. *IEEE J. Ocean Engineering*, 22(4):625–638, 1997.

[8] P. Moutarlier and R. Chatila. An experimental system for incremental environment modeling by an autonomous mobile robot. In *1st International Symposium on Experimental Robotics*, Montreal, June 1989.

[9] H. Singh. *An entropic framework for AUV sensor modelling*. PhD thesis, Massachusetts Institute of Technology, 1995.

[10] C. M. Smith and J. J. Leonard. A multiple hypothesis approach to concurrent mapping and localization for autonomous underwater vehicles. In *International Conference on Field and Service Robotics*, Sydney, Australia, 1997.

[11] C. M. Smith, J. J. Leonard, A. A. Bennett, and C. Shaw. Feature-based concurrent mapping and localization for autonomous underwater vehicles. In *IEEE Oceans*, 1997.

[12] R. Smith, M. Self, and P. Cheeseman. Estimating uncertain spatial relationships in robotics. In I. Cox and G. Wilfong, editors, *Autonomous Robot Vehicles*. Springer-Verlag, 1990.

[13] S. T. Tuohy, J. J. Leonard, J. G. Bellingham, N. M. Patrikalakis, and C. Chryssostomidis. Map based navigation for autonomous underwater vehicles. *International Journal of Offshore and Polar Engineering*, 6(1):9–18, March 1996.

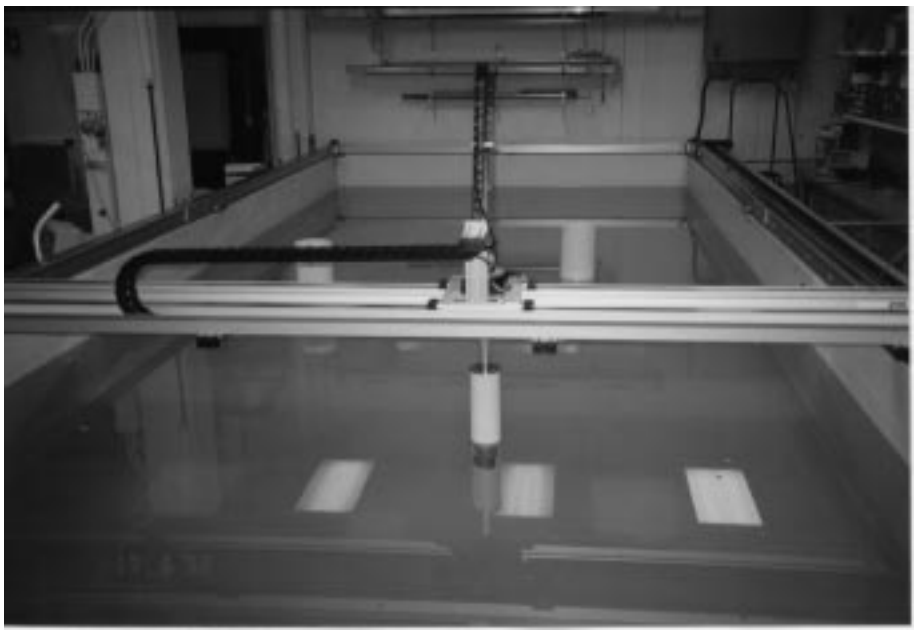

Figure 3: The planar robotic positioning system and sector-scan sonar used in the experiments.

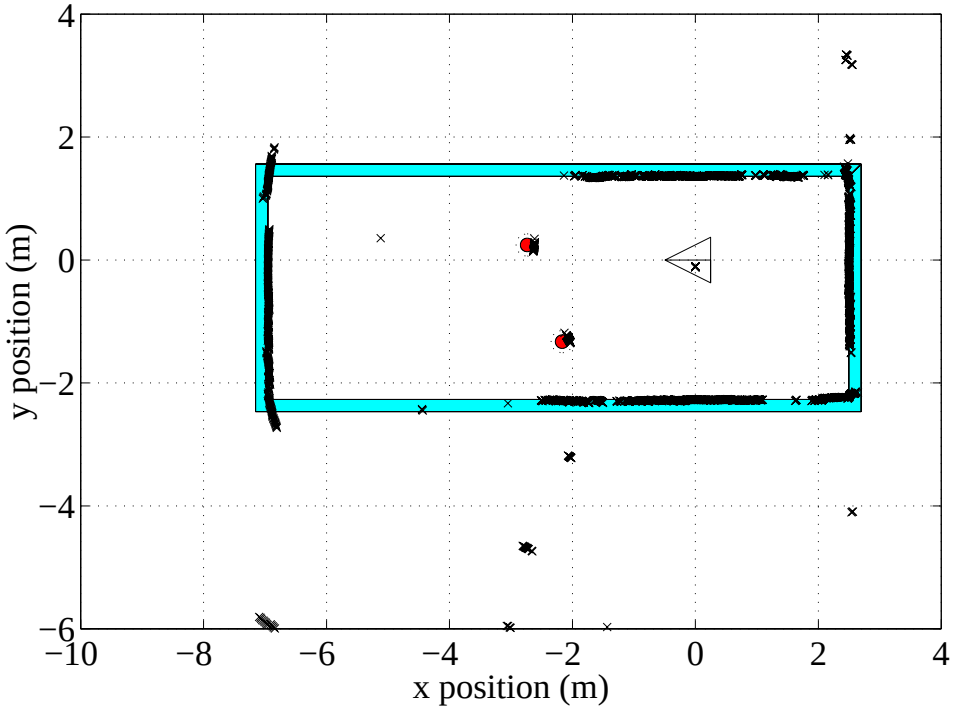

Figure 4: The returns from the sonar from a 360° scan of the tank from the origin. The crosses shows individual returns. The small circles identify the position of the features (PVC tubes), with a dotted 5 cm outside circle drawn around them to signify the minimum allowable distance between the sonar and the features. The sonar is mounted on the carriage of the positioning system, which serves as a "simulated AUV". The location of the sonar is shown by a triangle. The outline of the tank is shown in gray.